Research Article Vol. 3, No. 7 / July 2016 / Optica 702

Wide field-of-view fluorescent antenna for visible light communications beyond the étendue limit

Pavlos P. Manousiadis,[1] Sujan Rajbhandari,[2,3] Rahmat Mulyawan,[2] Dimali A. Vithanage,[1] Hyunchae Chun,[2] Grahame Faulkner,[2] Dominic C. O'Brien,[2] Graham A. Turnbull,[1,4] Stephen Collins,[2] and Ifor D.W. Samuel[1,5]

[1]Organic Semiconductor Centre, SUPA, School of Physics and Astronomy, University of St Andrews, St Andrews KY16 9SS, UK
[2]Department of Engineering Science, University of Oxford, Oxford OX1 3PJ, UK
[3]Current address: School of Computing, Electronics and Mathematics, Coventry University, Coventry CV1 2JH, UK
[4]e-mail: gat@st-andrews.ac.uk
[5]e-mail: idws@st-andrews.ac.uk

Received 4 April 2016; revised 19 May 2016; accepted 21 May 2016 (Doc. ID 262513); published 28 June 2016

Visible light communications (VLC) is an important emerging field aiming to use optical communications to supplement Wi-Fi. This will greatly increase the available bandwidth so that demands for ever-higher data rates can be met. In this vision, solid-state lighting will provide illumination while being modulated to transmit data. An important obstacle to realizing this vision are receivers, which need to be inexpensive, sensitive, fast, and have a large field of view (FoV). One approach to increasing the sensitivity of a VLC receiver is to increase the area of the receiver's photodetector, but this makes them expensive and slow. An alternative approach is to use optical elements to concentrate light, but conservation of étendue in these elements limits their FoV. In this paper, we demonstrate novel antennas that overcome these limitations, giving fast receivers with large collection areas and large FoV. Our results exceed the limit of étendue, giving an enhancement of light collection by a factor of 12, with FoV semi-angle of 60°, and we show a threefold increase in data rate.

Published by The Optical Society under the terms of the Creative Commons Attribution 4.0 License. Further distribution of this work must maintain attribution to the author(s) and the published article's title, journal citation, and DOI.

OCIS codes: (060.4510) Optical communications; (160.4890) Organic materials; (190.4360) Nonlinear optics, devices.
http://dx.doi.org/10.1364/OPTICA.3.000702

1. INTRODUCTION

Visible light communications (VLC) is a promising new paradigm for wireless communications, in which light from existing light sources is used as the data carrier [1,2]. Despite the relatively short time since its inception [3], VLC has already achieved higher data rates than comparable radio frequency (RF) communications systems [4,5]. The popularity of wireless communications means that RF bandwidth will not be enough to satisfy future user demands, and, hence, further increases in channel capacity will be essential. Like other communications systems, the maximum capacity of a VLC channel is determined by a combination of the bandwidth of the channel and the signal-to-noise ratio of the receiver. However, future VLC systems will use LEDs primarily designed to provide illumination as transmitters. Their bandwidths are limited to 20 MHz or less [6,7], and this makes achieving a high signal-to-noise ratio particularly important in VLC. In principle, a large receiver signal can be obtained by collecting a large fraction of the light from a transmitter. However, a large photodetector (e.g., photodiode) would normally be slow (limiting bandwidth [8]) and expensive. This means that the only way to increase the signal-to-noise ratio in a receiver is to concentrate light onto a photodetector using an optical element, such as a lens or a compound parabolic reflector (CPC). These optical elements are based upon reflection and refraction and therefore conserve étendue [see Fig. 1(a)]. This means that increasing the optical gain (the input area S_{in} divided by the output area S_{out}) of the element reduces its field of view (FoV) [9–11]. In particular, for optical elements with a refractive index n, the étendue-limited maximum possible gain [9,12] C_{max} is $n^2/\sin^2\theta$, where θ is the semi-angle that defines the FoV. This means that, for optical elements with a refractive index of 1.5 and a gain of 50, the FoV will be less than 12°, and will not be compatible with mobile devices such as smartphones and laptop computers. There is, therefore, a need to develop a convenient method of concentrating light from a relatively large area onto a photodetector, while maintaining a bandwidth of more than 20 MHz and a wide FoV.

In this paper, we present a novel approach to tackle this challenge and experimentally demonstrate a simple and inexpensive optical antenna that combines gain of more than 1 order of magnitude with a wide FoV of 60°, exceeding the limit set by the conservation of étendue. Our approach for VLC optical antennas is to use a thin layer of fluorescent material and glass cladding [see

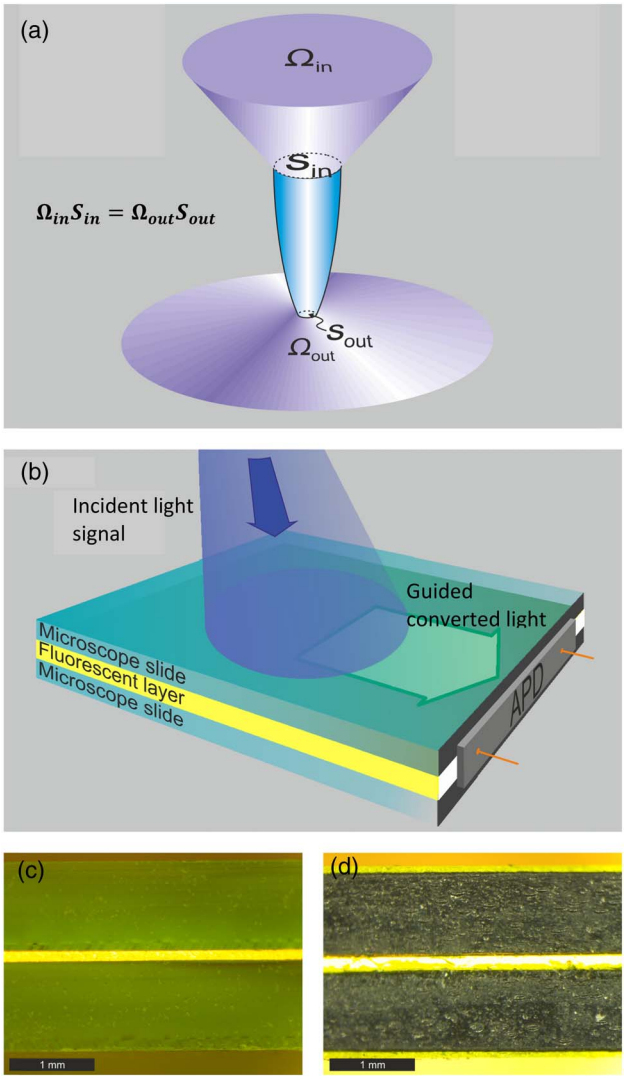

Fig. 1. Étendue and fluorescent antenna. (a) Schematic explanation of étendue conservation. The étendue for an optical system is defined as the product of the area of entrance or exit aperture (S) times the solid angle of acceptance or output (Ω). (b) Schematic representation of the fluorescent antenna. The yellow region consists of a layer of Cm6 in SU-8 coated with epoxy NOA68. APD denotes avalanche photodiode. (c) Photograph of antenna's edge. The thickness of SU-8 was ~15 μm. (d) Photograph of the edge of the antenna covered by masking tape so only light in the organic layer is detected.

Fig. 1(c)]. In these fluorescent antennas, a fluorescent material absorbs the incident light and re-emits it at a longer wavelength. Then, since the fluorescent material has a higher refractive index than its surrounding environment, part of the emitted light is retained inside it by total internal reflection (TIR). This light can then escape at the edge of the fluorescent antenna, where the photodetector of the receiver is placed. The achievable gain, in power density, from the edges can be significant, while the FoV follows closely a cosine law and so is approximately 60° (half-width at half-maximum). The reason the fluorescent antenna exceeds the étendue limit for gain is because it is based on fluorescence, which is accompanied by a Stokes shift, and not exclusively on refraction or reflection. In other words, the number of photons rather than the energy flux is conserved [10,11]. In this regard, they resemble luminescent solar concentrators that have been proposed as an inexpensive method of collecting solar energy [13–15]. A detailed description of the underlying physics can be found in Refs. [16–19]. Nevertheless, implementation of a fluorescent antenna for a communications system presents some difficult optical, material, and fabrication challenges [20].

2. FABRICATION AND PHOTOPHYSICS OF FLUORESCENT OPTICAL ANTENNAS

The main characteristics required for a good fluorescent antenna for VLC are: (i) a refractive index that will capture the emitted light in the layer of fluorescent material; (ii) strong absorption in the region of 450 nm matching the emission of GaN/InGaN LEDs, but weak re-absorption of its own fluorescence; (iii) high fluorescence quantum yield (PLQY); (iv) excited states with a lifetime of less than 10 ns; and (v) a thin fluorescent layer to enable small area photodetectors to be used, since the bandwidth of small photodetectors is broader [8].

Based on the above criteria, we selected the dye Coumarin 6 (Cm6) because of its high PLQY, absorption peaking in the blue region of the spectrum, and short fluorescence lifetime. However, as dyes suffer severe quenching of fluorescence at high concentrations, the Cm6 was dispersed in a host matrix. In particular, we explored two crosslinkable materials as hosts, the photoresist SU-8 and the epoxy NOA68. These were selected because they are simple to process, transparent in the wavelength range of interest, can co-dissolve Cm6, and give films with higher refractive index than glass, enabling them to be used to make waveguides with glass cladding.

To fabricate the antennas, a thin fluorescent film was sandwiched between two microscope slides (25 mm × 75 mm × 1.1 mm, $n = 1.52$) using UV curable epoxy NOA68 ($n = 1.54$). Two different structures were made. In one case, the yellow light waveguides in the combined SU-8 and NOA68 layers; in the other case, it waveguides in the NOA68 layer. The total thickness of the thin waveguiding layer, between the two microscope slides, was 100 μm. Some light will escape into the glass layers (microscope slides). For this reason, the edges of the glass slides were covered by black tape [see Fig. 1(d)], so that only light collected from the thin waveguiding layer would be detected at the edges of the antenna.

The photophysical properties of the dye Cm6 in the photoresist SU-8 are shown in Fig. 2. The properties of the dye in NOA68 are very similar and can be found in Supplement 1. In particular, Cm6 absorbs blue light strongly [see Fig. 2(a)], matching the emission band of the GaN/InGaN LEDs, typically used in solid-state lighting. This dye also emits in the green region of the spectrum, with peak wavelengths at 500 and 510 nm for concentrations of 0.01 and 3 mg/ml in a blend of SU-8, respectively [see Fig. 2(a)]. The higher concentration film has a more pronounced shoulder appearing at 540 nm. The difference in peak position and the shoulder appearance is due to self-absorption of the emitted light that occurs due to some overlap of the emission and absorption spectra on the short wavelength side of the emission. The key point is that, as shown in Fig. 2(b), the PLQY of these films remains high, between 80% and 95%, for concentrations up to 3 mg/ml. Furthermore, the stability of the film was verified by measuring the PLQY for a period of more than a month (see Supplement 1). In addition, Fig. 2(c) shows that the time-resolved fluorescence exhibits a single exponential decay with a lifetime of 3.1 ns. This means that the temporal response of

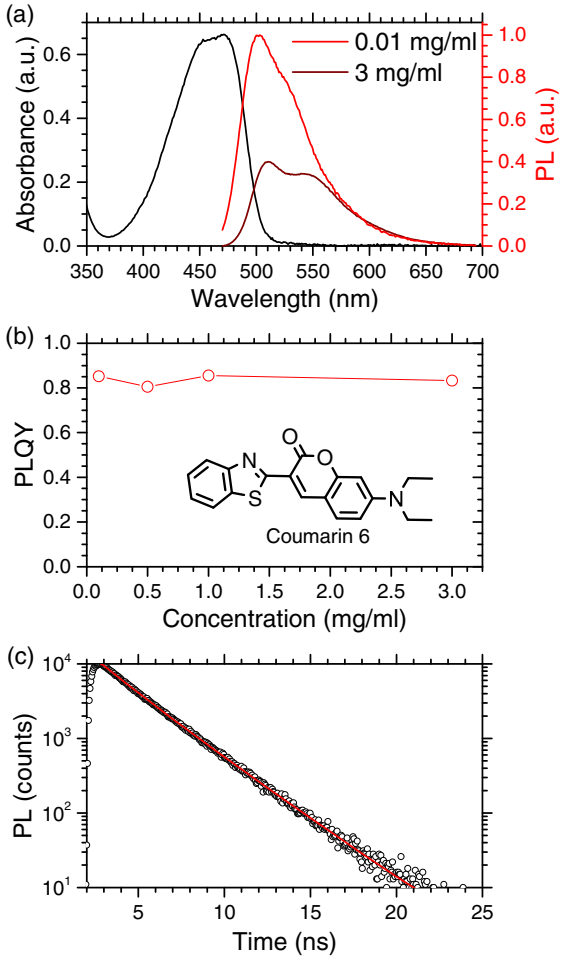

Fig. 2. Photophysics of Cm6 in SU-8. (a) Absorption and emission spectra (excited at 450 nm) of films made from Cm6 in SU-8. (b) Dependence of PLQY on concentration of Cm6 in SU-8. The inset shows the molecular structure of Cm6. (c) Photoluminescence (PL) versus time measurements, following excitation at 393 nm.

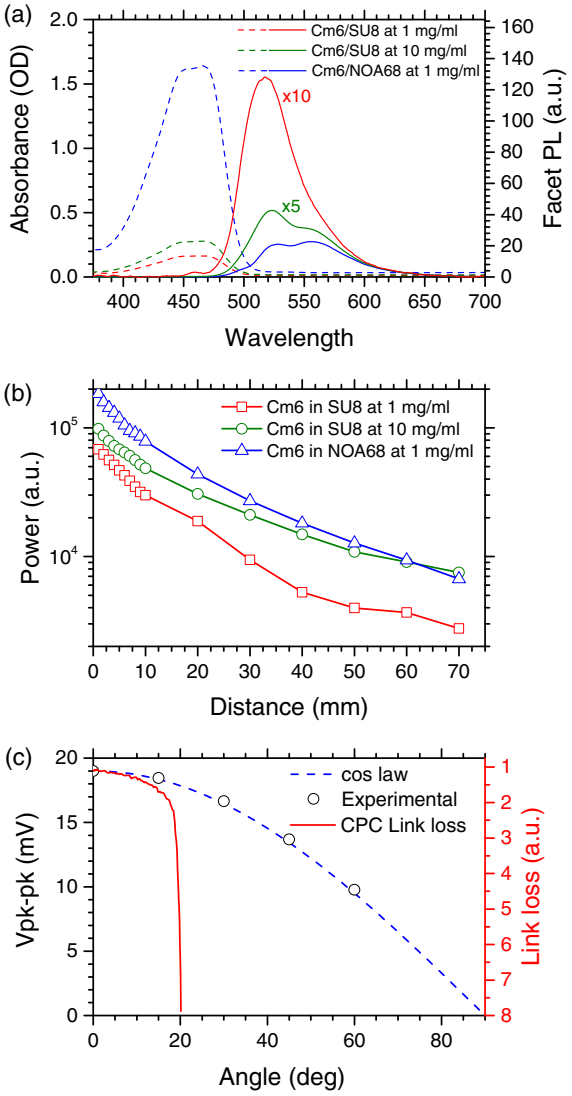

Fig. 3. Optical properties of fluorescent antennas deposited from solutions with concentrations as marked. (a) Absorption and facet PL emission spectra of antennas. (b) Attenuation of the collecting power as a function of distance from the collection edge. (c) FoV of the antenna of Cm6 in NOA68 at 1 mg/ml. For comparison, the dashed line shows the cosine law, while the red line shows the FoV of a CPC with similar gain.

the Cm6 is much faster than the typical LED modulation rate and will not limit the bandwidth of the VLC communications channel.

3. OPTICAL CHARACTERIZATION

To understand the performance and optimize the fabrication parameters, the optical properties of the antennas were investigated, and the results are presented in Fig. 3. As the absorption and emission spectra are very important for antenna operation, we measured them on the actual antenna structure, collecting the emission from the edge. The results, shown in Fig. 3(a), are similar to the materials measurements presented in Fig. 2(a). Experimentally (see Table 1), it was found that the gain of the antenna increased as the optical density of the fluorescent layer increased. For this reason, the optical density was initially increased by using a higher concentration of Cm6 in SU-8. However, this approach was limited by concentration quenching, and so Cm6 was instead mixed directly with the NOA68. The Photoluminescence (PL) emission from the edge of the antennas also shows the characteristics identified in the photophysical investigation. In particular, as the optical density of the fluorescent layer increases, the shoulder becomes more pronounced.

Another important fabrication parameter that determines the useful antenna length is attenuation loss. Figure 3(b) shows the relative fluorescence power detected at the edge of the antenna as a function of the distance of excitation from the edge. Propagation losses in the waveguide lead to an attenuation of the fluorescence that shows a complex exponential decay. We attribute this to the loss of nonguided rays at short distances, isotropic emission in the plane, and the change in absorption as the light propagates through the fluorescent layer due to self-absorbance and the resulting shift in spectra. As shown in Fig. 3(b), the use of the optically dense antenna results in more power being collected at the antenna edge. At the same time, however, as can be seen from Fig. 3(a), there is stronger self-absorption of short wavelengths. Table 1 summarizes the gain of the samples, when measured

Table 1. Summary of Fluorescent Antenna Properties

Sample	OD at 450 nm	Gain	BW (MHz)
Cm6/SU-8 at 1 mg/ml	0.16	4	50.2
Cm6/SU-8 at 10 mg/ml	0.27	6	50.0
Cm6/NOA68 at 1 mg/ml	1.61	12	41.0

under flood illumination, i.e., when the whole sample is illuminated, by a blue 450 nm LED.

The FoV was measured by placing the antenna and attached photodiode on a rotation stage. The sample was flood illuminated with collimated light from a blue LED, and the received signal was recorded as a function of the excitation angle. The results for these FoV measurements [see Fig. 3(c)] show that the received power at the edge of the antenna falls away with incidence angle, following a cosine dependence. This shows that the dominant phenomenon that determines the FoV is the projected area of the antenna, i.e., a cosine law, and the FoV, therefore, has a semi-angle of 60°. Table 1 summarizes the gain of the samples, when measured under flood illumination, i.e., when the whole sample is illuminated, by a blue 450 nm LED. At normal incidence, the measured gain of the most optically dense antenna was 12, which is more than 4 times higher than the maximum theoretical gain of an optical, étendue-limited, concentrator with a similar FoV. In comparison, the FoV of a compound parabolic concentrator [21], with a gain similar to that of the fluorescent antenna [also presented in Fig. 3(c)], would be 20°.

4. COMMUNICATION CHARACTERIZATION

In a communication system, the achievable data rates are proportional to the system bandwidth (BW), at a specific signal-to-noise ratio. We therefore measured the BW as a function of excitation distance from the edge with the detector, and the results are presented in Fig. 4(a). It can be seen that there is a steady decrease in BW with excitation distance, which eventually saturates, as the distance increases. We attribute this variation in bandwidth to self-absorption of the emitted light. In particular, the absorption and re-emission of photons have the effect of increasing the effective PL lifetime, resulting in a lower BW (see Supplement 1). Nonetheless, in all cases, the 3 dB electrical bandwidths were above 40 MHz, which is significantly higher than the BW of most commercially available LEDs designed for illumination, which is typically in the range of 5–20 MHz [6,7].

Finally, the possibility of creating a communication link using a fluorescent antenna was investigated. A pseudo-random binary sequence was translated into voltage variations using an arbitrary waveform generator, and used to modulate the light output of a commercial blue LED. The modulation scheme that was used was on–off keying (OOK), where the absence of light represents bits with a value of zero and full intensity represents bits with a value of 1. In these experiments, a circular avalanche photodiode (APD) with active area of 1 mm^2, followed by a transimpedance amplifier, was used as the photodetector. The data rates, achieved in a 0.5 m long data link, are presented in Fig. 4(b). In this figure, two cases are compared: one where the APD was excited directly, and the other where the APD received light from the edge of the fluorescent antenna. In both cases, the FoV was 60°. To have the same illuminated area of APD, a 100 μm metallic slit was used in front of the APD in the case of direct excitation. An important

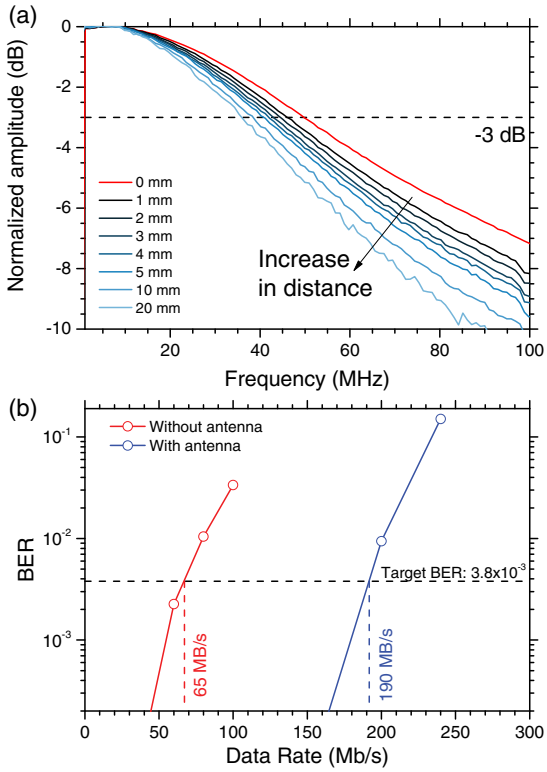

Fig. 4. Communication link using a fluorescent antenna. (a) Results of BW measurement for different distances of the excitation from the edge of the sample. (b) Comparison between the achievable data rates using OOK, with and without a fluorescent antenna.

characteristic of a communications system is how the bit error rate (BER), defined as the number of error bits divided by the total number of bits, depends upon the data rate. The results of BER measurements are shown in Fig. 4(b). As forward error correction can work well at error rates of up to 3.8×10^{-3}, the data rate of the system at BER is of particular interest [4,22]. For the APD alone, at this BER, the data rate is 65 Mb/s, and this increases to 190 Mb/s when the fluorescent antenna is used. This shows that an almost threefold improvement in the data rate can be achieved, without decreasing the FoV.

5. CONCLUSIONS

In conclusion, we have demonstrated a new category of simple and inexpensive optical antennas for VLC. Our fluorescent antennas overcome the limitations created by the conservation of étendue in refractive–reflective-based optical systems, giving a large signal gain, combined with a large FoV. Specifically, we demonstrated a gain of 12 combined with a huge FoV, with a full width at half-maximum of 120°. Nevertheless, the achieved gain, although significantly higher than a conventional optical element, is well below the upper bound arising from thermodynamic considerations [10,11]. Hence, it should be possible to improve the performance of our optical antennas in the future. In addition, we have demonstrated the importance of the new optical antennas for free-space optical communications by showing a threefold enhancement of data transmission rate. Since these antennas are inexpensive and thin, they could be easily

incorporated in mobile phones, tablets, computers, and even clothing to enable rapid mobile communication.

The research data supporting this publication can be accessed at [23].

Funding. Engineering and Physical Sciences Research Council (EPSRC) (EP/I00243X, EP/K00042X, EP/K008757); European Research Council (ERC) (321305); Royal Society; Wolfson Foundation.

Acknowledgment. IDWS is the recipient of a Royal Society Wolfson Research Merit Award.

See Supplement 1 for supporting content.

REFERENCES

1. O. Ergul, E. Dinc, and O. B. Akan, "Communicate to illuminate: state-of-the-art and research challenges for visible light communications," Phys. Commun. **17**, 72–85 (2015).
2. D. Karunatilaka, F. Zafar, V. Kalavally, and R. Parthiban, "LED based indoor visible light communications: state of the art," IEEE Commun. Surv. Tutorials **17**, 1649–1678 (2015).
3. T. Komine and M. Nakagawa, "Fundamental analysis for visible-light communication system using LED lights," IEEE Trans. Consum. Electron. **50**, 100–107 (2004).
4. D. Tsonev, C. Hyunchae, S. Rajbhandari, J. J. D. McKendry, S. Videv, E. Gu, M. Haji, S. Watson, A. E. Kelly, G. Faulkner, M. D. Dawson, H. Haas, and D. O'Brien, "A 3-Gb/s single-LED OFDM-based wireless VLC link using a gallium nitride μLED," IEEE Photon. Technol. Lett. **26**, 637–640 (2014).
5. H. Chun, S. Rajbhandari, G. Faulkner, D. Tsonev, E. Xie, J. McKendry, E. Gu, M. Dawson, D. C. O. Brien, and H. Haas, "LED based wavelength division multiplexed 10 Gb/s visible light communications," J. Lightwave Technol. (to be published).
6. J. Grubor, S. C. J. Lee, K.-D. Langer, T. Koonen, and J. W. Walewski, "Wireless high-speed data transmission with phosphorescent white-light LEDs," in *33rd European Conference and Exhibition of Optical Communication* (VDE Verlag, 2007), post-deadline paper.
7. H. Chun, S. Rajbhandari, G. Faulkner, and D. O'Brien, "Effectiveness of blue-filtering in WLED based indoor visible light communication," in *3rd International Workshop in Optical Wireless Communications (IWOW)* (2014), pp. 60–64.
8. See, for example, "Si APD, S12023 series," etc. (Hamamatsu, 2014).
9. W. T. Welford and R. Winston, *Optics of Nonimaging Concentrators: Light and Solar Energy* (Academic, 1978).
10. H. Ries, "Thermodynamic limitations of the concentration of electromagnetic radiation," J. Opt. Soc. Am. **72**, 380–385 (1982).
11. G. Smestad, H. Ries, R. Winston, and E. Yablonovitch, "The thermodynamic limits of light concentrators," Sol. Energy Mater. **21**, 99–111 (1990).
12. R. Winston, J. C. Miñano, and P. G. Benitez, *Nonimaging Optics* (Academic, 2005).
13. W. G. J. H. M. van Sark, K. W. J. Barnham, L. H. Slooff, A. J. Chatten, A. Büchtemann, A. Meyer, S. J. McCormack, R. Koole, D. J. Farrell, R. Bose, E. E. Bende, A. R. Burgers, T. Budel, J. Quilitz, M. Kennedy, T. Meyer, C. D. M. Donegá, A. Meijerink, and D. Vanmaekelbergh, "Luminescent solar concentrators: a review of recent results," Opt. Express **16**, 21773–21792 (2008).
14. M. G. Debije and P. P. Verbunt, "Thirty years of luminescent solar concentrator research: solar energy for the built environment," Adv. Energy Mater. **2**, 12–35 (2012).
15. M. J. Currie, J. K. Mapel, T. D. Heidel, S. Goffri, and M. A. Baldo, "High-efficiency organic solar concentrators for photovoltaics," Science **321**, 226–228 (2008).
16. J. S. Batchelder, A. H. Zewai, and T. Cole, "Luminescent solar concentrators. 1: theory of operation and techniques for performance evaluation," Appl. Opt. **18**, 3090–3110 (1979).
17. J. S. Batchelder, A. H. Zewail, and T. Cole, "Luminescent solar concentrators. 2: experimental and theoretical analysis of their possible efficiencies," Appl. Opt. **20**, 3733–3754 (1981).
18. P. Kittidachachan, L. Danos, T. J. J. Meyer, N. Alderman, and T. Markvart, "Photon collection efficiency of fluorescent solar collectors," CHIMIA Int. J. Chem. **61**, 780–786 (2007).
19. H. Sträter, S. Knabe, T. J. J. Meyer, and G. H. Bauer, "Spectrally and angle-resolved emission of thin film fluorescence collectors," Prog. Photovoltaics **21**, 554–560 (2013).
20. S. Collins, D. C. O'Brien, and A. Watt, "High gain, wide field of view concentrator for optical communications," Opt. Lett. **39**, 1756–1759 (2014).
21. D. O'Brien, R. Turnbull, M. H. Le, G. Faulkner, O. Bouchet, P. Porcon, M. El Tabach, E. Gueutier, M. Wolf, L. Grobe, and L. Jianhui, "High-speed optical wireless demonstrators: conclusions and future directions," J. Lightwave Technol. **30**, 2181–2187 (2012).
22. "Forward error correction for high bit-rate DWDM submarine systems," ITU-T Recommendation G.975.971, 2004.
23. http://dx.doi.org/10.17630/d6ae5a33-c93d-4e83-86e5-fcb39ff07350.

163.1.203.194 (to 2018-01-17 10:28:24)